scientific reports

Check for updates

OPEN

Unconventional phonon blockade effect in array of three coupled weakly nonlinear nanomechanical resonators

Bhaskar Kumar & Prabhu Rajagopal✉

Phonon antibunching, a phenomenon arising from the quantum statistics of mechanical vibrations, has attracted significant attention due to its potential applications in quantum information processing, sensing, and energy harvesting. Here, we present a comprehensive investigation of phonon antibunching in a system consisting of three weakly nonlinear coupled nanomechanical resonators. We analytically derive and study the antibunching behavior of phonons in the proposed system and bring insight into the underlying mechanisms. The optimal phonon blockade results from destructive quantum interference due to distinct two-phonon excitation pathways. Due to this quantum interference, these unconventional phonon blockade systems can achieve antibunched statistics even in weakly nonlinear regimes, in contrast to conventional phonon blockade systems that require strong nonlinearity. We show that with the inclusion of an additional resonator, there are multiple additional two-phonon excitation pathways compared to two resonator cases, which results in stronger phonon antibunching and supports single phonon for longer duration. These findings are interesting for practical phononics using coupled-resonator systems.

Phonons are quanta of lattice vibrations crucial in transporting and manipulating mechanical energy in various physical systems, including solid-state materials, nanoscale devices, and microelectromechanical systems (MEMS). While much progress has been made in the study of quantum phenomena involving photons, electrons, and atoms, there is a growing interest in exploring the quantum nature of mechanical vibrations[1–4].

Coupled resonator systems have emerged as a versatile platform for investigating the quantum properties of phonons[5,6]. These systems consist of multiple mechanical resonators or acoustic cavities coupled through mechanical interactions or phonon tunneling. The strong coupling between the resonators allows for the coherent exchange of phonons, enabling the exploration of various intriguing phenomena, including antibunching.

In recent years, cavity optomechanics has been a significant area of study, where the motional degrees of freedom of a mechanical oscillator are coupled to optical fields inside the cavity. This results in a true two-way interaction between electromagnetic field inside an optical cavity and the oscillator displacement[7,8]. The excellent coupling makes cavity optomechanical systems exquisite candidates for potential uses in quantum information processing[9,10], quantum communication, quantum sensors, etc.[11]. Recent advances in ground state cooling experiments have opened new doors for potential applications of cavity optomechanics by enabling the realization of mechanical resonators near the ground state[12–14]. Currently, almost all experiments of cavity optomechanics are based on linearized single photon-phonon interactions. However, the intrinsic nature of interaction in the strong coupling regime is nonlinear. This has led to much interest in nonlinear optics, including the generation of non-Gaussian states[15], photon blockade effects[16], nonclassical state of antibunched mechanical resonators[17]. Nonclassical light, a necessary component of quantum information and communication, has been produced by nonlinear coupling of optomechanical systems[18].

Antibunching is a phenomenon that arises from the quantum statistics of Bosonic particles such as photons and phonons, with this paper focusing on the latter. Under phonon antibunching, the probability of simultaneously detecting two quanta of phonons is suppressed compared to what would be expected for a classical distribution. This phenomenon, also termed as the Phonon blockade effect (PBE), has significant implications for the generation and manipulation of quantum states of mechanical motion and applications in quantum information processing and sensing. Nonlinearity is required to realize the phonon blockade effect. It can be either intrinsic or realized by coupling the mechanical resonator to an ancillary two-level system (qubit or two-level defects) assuming far off-resonant interactions[19–21]. The latter can be a Kerr-type third-order $\chi^{(3)}$[6,21,22]

Indian Institute of Technology Madras, Chennai 600036, India. ✉email: prajagopal@iitm.ac.in

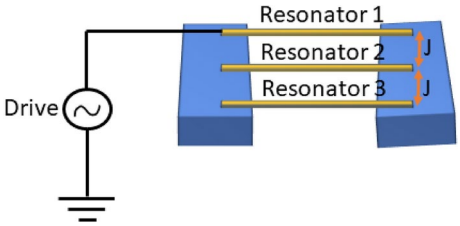

Fig. 1. Schematic of the proposed system consisting of three coupled weakly nonlinear mechanical resonators, one of which is driven. J is the coupling strength between the resonators.

or second-order $\chi^{(2)}$[23,24] nonlinearity or Duffing type nonlinearity. The Duffing nonlinearity can be induced in a spin-mechanical system where a nanomechanical resonator is magnetically coupled to a single nitrogen-vacancy (NV) center[25].

Two approaches are commonly used to achieve phonon antibunching, namely the conventional and unconventional phonon blockade effects (CPB and UPB, respectively). CPB draws parallels from conventional photon blockade effects[26–28] and relies on stronger nonlinearity with respect to the decay rate of the system to suppress the two phonon excitation states. The strong nonlinearity results in anharmonic energy levels in the resonator where the two phonon states will be blockaded at larger detuning after the first phonon is excited by an external field. CPBs with such principles have been studied in NAMRs coupled to a qubit[20], quadratically coupled optomechanical systems[29] or spin qubits nonlinearly coupled to phonons[30]. The nonlinearity required to observe antibunching behavior is very high for the case of CPB. However, the typical intrinsic nonlinearity is weak, and strong nonlinearities are challenging to realize. Recently, unconventional photon blockade has been predicted in the regime of weak nonlinearities in which strong photon antibunching can be observed via destructive quantum interference[31–35]. Similarly, UPBs are explored for phonons, which can be realized even in weak nonlinear regimes due to quantum interference effects. In the case of UPB, the presence of two phonons in the system is mitigated by the destructive quantum interference between different excitation pathways from the ground to the two-phonon state[5,36,37]. Phonon blockades have also been proposed in hybrid systems[38–40]. Similar to CPB, sub-Poissonian phonon statistics are expected from UPB. Our group has shown UPB in a coupled resonator system with its prospective realization in a hermetically sealable device at near-micron dimensions and milliKelvin temperatures[41]. Here, we study the effect of an array of three coupled resonator systems on the UPB, with the goal of exploring better antibunching performance.

Results

Model and hamiltonian

We consider a three-mode system where three weakly nonlinear NAMRs are suspended, one above the other. The resonators are clamped on both sides and coupled to each other through Coulomb interaction. A schematic of the proposed system is given in Fig. 1. We consider one of the resonators to be driven.

The Hamiltonian of the system can be broken into four parts as follows:

$$H = H_{free} + H_{nl} + H_{co} + H_{drive}, \tag{1}$$

where H_{free} is the free Hamiltonian of all the resonators combined, H_{nl} is the Hamiltonian describing Kerr nonlinearity U in all the three mechanical resonators and H_{co} represents Coulomb-coupled interaction between the resonators. The corresponding terms are given as:

$$H_{\text{free}} = \omega_m \left(\sum_{i=1}^{n} b_i^\dagger b_i \right) \tag{2}$$

where $b_i(b_i^\dagger)$ are the annihilation (creation) operators for the i_{th} mechanical resonator modes and ω_m is the resonant frequency of the mechanical modes. The nonlinearity Hamiltonian is given by:

$$H_{nl} = \sum_{i=1}^{n} U \left(b_i^\dagger + b_i \right)^4 \tag{3}$$

where U is the nonlinearity in all the mechanical resonators. Similarly, the coupling Hamiltonian is given by:

$$H_{co} = \sum_{i=1}^{n} \sum_{j=1}^{n} J_{ij} \left(b_i^\dagger + b_i \right) \left(b_j^\dagger + b_j \right) \tag{4}$$

where J_{ij} is the coupling strength between the ith and the jth resonator respectively. The term J_{ij} depends on the potential energy U_{ij}, masses (m_i, m_j) and resonant frequency ω_m by the following equation[37,42,43]:

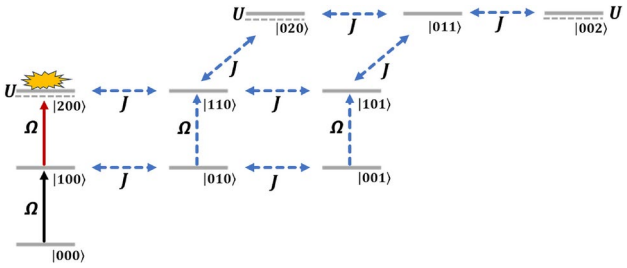

Fig. 2. Energy level diagrams of states under the Hamiltonian.

$$J_{ij} = \frac{1}{2}\frac{d^2U_{ij}^e}{dz^2}\sqrt{\frac{1}{m_1 m_2 \omega_m^2}} \tag{5}$$

In the weak coupling regime, considering only the resonant terms the Coulomb interaction Hamiltonian reduces to[5]:

$$H_{co} = \sum_{i}^{n-1}\sum_{j=i+1}^{n} J_{ij}\left(b_i^\dagger b_j + b_j^\dagger b_i\right) \tag{6}$$

The three mechanical modes are given by pumps with frequencies ω_1, ω_2, and ω_3 with corresponding pump amplitudes Ω_1, Ω_2 and Ω_3 described in the term H_{drive}.We assume that $\omega_1 = \omega_2 = \omega_3 = \omega_p$.

$$H_{\text{drive}} = \sum_{j=1}^{n}\Omega_j\left(b_j^\dagger e^{-i\omega_p t} + b_j e^{i\omega_p t}\right) \tag{7}$$

Using rotating wave approximation, H_{nl} can also be simpified:

$$H_{nl} = \sum_{i=1}^{n} U\left(b_i^\dagger b_i^\dagger b_i b_i\right) \tag{8}$$

Thus, the Hamiltonian describing the mechanical resonators in the frame rotating with the mechanical drive frequency assuming that only one of the resonators is driven so that $\Omega_2 = \Omega_3 = 0$ and $\Omega_1 = \Omega$ is given by:

$$H' = \Delta b_1^\dagger b_1 + \Delta b_2^\dagger b_2 + \Delta b_3^\dagger b_3 + U b_1^\dagger b_1^\dagger b_1 b_1 + U b_2^\dagger b_2^\dagger b_2 b_2 + U b_3^\dagger b_3^\dagger b_3 b_3 + J\left(b_1^\dagger b_2 + b_1 b_2^\dagger + b_2^\dagger b_3 + b_2 b_3^\dagger\right) + \Omega\left(b_1^\dagger + b_1\right) \tag{9}$$

where Δ is detuning from the mechanical pump frequency, $\omega_m - \omega_p$. Here, we have further assumed that the coupling of resonator 1 and resonator 3 is negligible compared to the coupling of resonator 1 to resonator 2 and similarly resonator 2 to resonator 3. This assumption is valid in our proposed scheme of stacking resonators one above the other as the separation between resonator 1 and resonator 3 would be large compared to the other two.

Phonon blockade with single drive: analytical study

We consider the energy level diagram of the system at low temperature and weak driving field ($\Omega << \gamma$) as shown in Fig. 2. Hence, we can assume that only the lower energy states of the system are occupied. We represent the state of the system with the ansatz wavefunction by truncating the Hilbert state of the system to n=2:

$$|\psi\rangle = C_{000}|000\rangle + C_{001}|001\rangle + C_{100}|100\rangle + C_{010}|010\rangle + C_{002}|002\rangle + C_{101}|101\rangle + C_{011}|011\rangle + C_{110}|110\rangle + C_{200}|200\rangle + C_{020}|020\rangle \tag{10}$$

with $C_{n_{b1}n_{b2}n_{b3}}$ being the probability amplitude for the corresponding state $|n_{b1}n_{b2}n_{b3}\rangle$. Now, to determine these coefficients we substitute the ansatz for the state into the Schrödinger equation $i\frac{\mathrm{d}|\psi\rangle}{\mathrm{d}t} = H_{\text{non}}|\psi\rangle$ where H_{non} is the non-Hermitian Hamiltonian $H_{\text{non}} = H' - \frac{i\gamma}{2}b_1^\dagger b_1 - \frac{i\gamma}{2}b_2^\dagger b_2 - \frac{i\gamma}{2}b_3^\dagger b_3$ to obtain a set of evolution equations for the coefficients $C_{n_{b1}n_{b2}n_{b3}}$ from which the optimal conditions can be obtained. The details of the procedure is given in the Method section.

Numerical method

The evolution of an open quantum system is given by Lindblad master equation of the form:

$$\frac{\mathrm{d}\rho}{\mathrm{d}t} = \mathscr{L}(\rho), \tag{11}$$

where L is the Liouvillian of the form:

$$\mathscr{L}(\rho) = -i\left[H', \rho\right] + \mathscr{D}(\rho) \tag{12}$$

Here $\mathscr{D}$ is the dissipator of the system which is of the form:

$$\mathscr{D}(\rho) = \sum_k \gamma_k \left[L_k \rho L_k^\dagger - \frac{1}{2}\left\{L_k^\dagger L_k, \rho\right\}\right] \tag{13}$$

For the case of harmonic oscillator subject to finite temperature bath, the dissipator is given by:

$$\mathscr{D}(\rho) = \gamma(\bar{n}+1)\left[b\rho b^\dagger - \frac{1}{2}\left\{b^\dagger b, \rho\right\}\right] + \gamma\bar{n}\left[b^\dagger \rho b - \frac{1}{2}\left\{bb^\dagger, \rho\right\}\right] \tag{14}$$

Thus, for the proposed system the master equation describing the time evolution of density matrix is given by:

$$\dot{\rho} = -i\left[H', \rho\right] + \gamma\left(n_{\mathrm{th},1}+1\right)L\left[b_1\right]\rho + \gamma n_{\mathrm{th},1} L\left[b_1^\dagger\right]\rho + \gamma\left(n_{\mathrm{th},2}+1\right)L\left[b_2\right]\rho + \gamma n_{\mathrm{th},2} L\left[b_2^\dagger\right]\rho + \gamma\left(n_{\mathrm{th},3}+1\right)L\left[b_3\right]\rho + \gamma n_{\mathrm{th},3} L\left[b_3^\dagger\right]\rho \tag{15}$$

where $L\left[b_i\right]\rho = b_i\rho b_i^\dagger - \frac{1}{2}b_i^\dagger b_i\rho - \frac{1}{2}\rho b_i^\dagger b_i$ is the Liouvillian operator for the mode b_i, H' is the effective Hamiltonian in rotating frame of reference (Eq. 9) and $n_{\mathrm{th,i}}$ denotes thermal phonon number at thermal bath temperature, T given by $n_{\mathrm{th,i}} = 1/\left[\exp\left(\omega_m/k_B T\right) - 1\right]$ We consider $n_{th,1} = n_{th,2} = n_{th,3}$. The master equation is solved numerically using the methods described in[44]. We calculate $g_{b1}^{(2)}(0)$ numerically by solving:

$$g_{b1}^{(2)}(0) = \frac{\mathrm{Tr}\left(\widehat{b_1}^+\widehat{b_1}^+\widehat{b_1}\widehat{b_1}\widehat{\rho}_{ss}\right)}{\mathrm{Tr}\left(\widehat{b_1}^+\widehat{b_1}\widehat{\rho}_{ss}\right)^2} \tag{16}$$

$g_{b1}^{(2)}(0)$ indicates probability of occupation of two phonons in the mechanical mode b_1 at the same time and approaches value of zero at phonon blockade.

Model validation

First, we plot the second-order correlation function, $g_{b1}^{(2)}(0)$ in Fig. 3a for the case of two resonator system at optimal values of nonlinearity U_{opt} corresponding to J/γ values of 1.5, 2.0 and 2.5 respectively. The choice of parameters is inspired by experimental work in cavity optomechanics[45,46]. Thus, it is within the expectation of the authors that the proposed system has a reasonable prospective experimental realization. The values of U_{opt} are obtained from an iterative procedure prescribed by Bamba et al.[47] in connection with photon blockade. The analytical expressions for U_{opt} and Δ_{opt} for fixed values of J and γ are given by:

$$\Delta_{\mathrm{opt}} = \pm\frac{1}{2}\sqrt{\sqrt{9J^4 + 8\gamma^2 J^2} - \gamma^2 - 3J^2},\ U_{\mathrm{opt}} = \frac{\Delta_{\mathrm{opt}}\left(5\gamma^2 + 4\Delta_{\mathrm{opt}}^2\right)}{2\left(2J^2 - \gamma^2\right)} \tag{17}$$

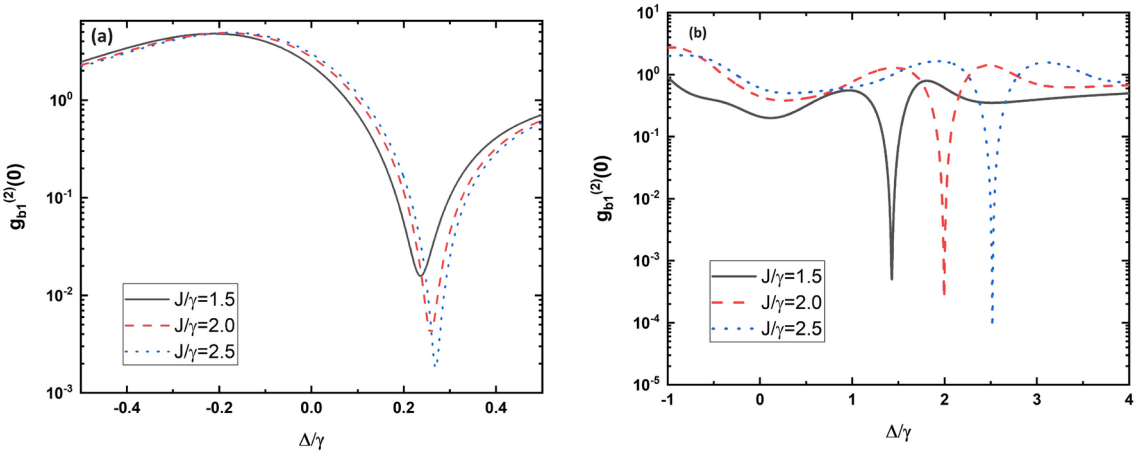

Fig. 3. (**a**) Plot of second order correlation function $g_{b1}^{(2)}(0)$ as a function of normalized detuning Δ/γ for different values of J/γ for a two resonator system. (**b**) Plot of second order correlation function $g_{b1}^{(2)}(0)$ as a function of normalized detuning Δ/γ for different values of J/γ for our proposed three resonator system.

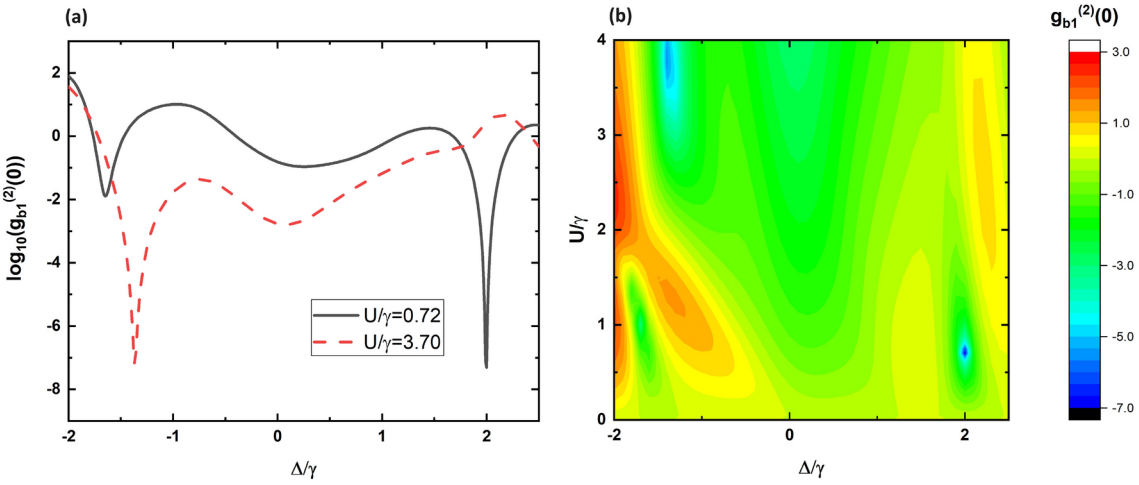

Fig. 4. (**a**) Plot of second order correlation function $log_{10}(g_{b1}^{(2)}(0))$ as a function of normalized detuning Δ/γ for different values of $U/\gamma = U_{opt}$ given by analytical computations for our proposed three resonator system, and (**b**) Contour Plot of $log_{10}(g_{b1}^{(2)}(0))$ as functions of normalized U and Δ Parameters: $\Omega = 0.01\gamma$ and

The optimal Δ_{opt}/γ values are given by these analytical expressions for J/γ values of 1.5, 2.0, and 2.5 are 0.24, 0.26, and 0.27, respectively. The corresponding $U = U_{opt}/\gamma$ values are 0.18, 0.09 and 0.06, respectively. Using numerical simulation, we plotted $g_{b1}^{(2)}(0)$ at $U = U_{opt}/\gamma$ for each J/γ. It is evident from Fig. 3a that strong phonon antibunching occurs at Δ_{opt}/γ values given by the analytical expression. Thus, our model and the numerical simulation based on it are in strong agreement with analytical results given by Bamba et al.[47], providing cross-verification for our approach.

Phonon antibunching

Next, using the thus-verified analytical model for our three resonator proposed system (described in the previous section), the optimal conditions for the phonon blockade are calculated for the same values of normalized coupling rate, i.e., for J/γ values of 1.5, 2.0, and 2.5, respectively: $J/\gamma = 1.5$: $(U/\gamma = 1.55, \Delta/\gamma = 1.428)$, $(U/\gamma = 5.22, \Delta/\gamma = -1.09)$ $J/\gamma = 2$: $(U/\gamma = 0.72, \Delta/\gamma = 1.995)$, $(U/\gamma = 3.7, \Delta/\gamma = -1.36)$ $J/\gamma = 2.5$: $(U/\gamma = 0.48, \Delta/\gamma = 2.52)$, $(U/\gamma = 0.66, \Delta/\gamma = -2.031)$, $(U/\gamma = 2.00, \Delta/\gamma = -2.30)$, $(U/\gamma = 3.84, \Delta/\gamma = -1.68)$

Using numerical methods, we plot the normalized equal time second-order correlation function, $g_{b1}^{(2)}(0)$ in Fig. 3b for the corresponding values of J/γ and U_{opt}/γ given by analytical results. As we can see from the figure, complete phonon antibunching is observed at the values of Δ/γ given by the optimal conditions as predicated from our analytical model. This complete antibunching is due to quantum interference that happens as a result of distinct pathways that interfere destructively, resulting in the complete suppression of two phonon excitations in resonator 1. To see this, consider the two phonon excitation pathways in the energy level diagram of Fig. 2a direct excitation path (solid red arrow) : $|100\rangle \xrightarrow{\Omega} |200\rangle$ and (b) tunnel-mediated transition pathways (dashed blue arrows): like $|100\rangle \overset{J}{\leftrightarrow} |010\rangle \xrightarrow{\Omega} (|110\rangle \overset{J}{\leftrightarrow} |101\rangle) \xrightarrow{J} |200\rangle$, among others. This leads to quantum interference under appropriate conditions which results in unconventional phonon blockade effect. The introduction of additional resonator results in multiple additional two-phonon excitation pathways compared to the two resonator case. This results in observance of stronger phonon blockade in our system as compared to the system with two coupled resonators (Fig. 3). The optimal parameters taken for the simulations are $U = U_{opt}/\gamma$= 1.55, 0.72 and 0.48 for J/γ = 1.5, 2.0 and 2.5 respectively.

For better visualization of the phonon blockade effect, the logarithmic $g_{b1}^{(2)}(0)$ values are plotted for all the solutions for J/γ in Fig. 4a and the corresponding contour color plots of $log_{10}(g_{b1}^{(2)}(0))$ is plotted as a functions of normalized cavity detuning, Δ/γ and normalized nonlinearity strength, U/γ are presented in Fig. 4b. Similar contour color plots are shown in Fig. 5a and b for the case of $J/\gamma = 1.5$ and $J/\gamma = 2.5$ respectively. All these plots show that phonon antibunching occurs at the values predicted by the analytical calculations.

The delayed second-order correlation function is plotted in Fig. 6a as a function of normalized time delay $\tau/(2\pi/J)$. $g_{b1}^{(2)}(\tau)$ indicates the probability of detecting a second phonon at time $t + \tau$ after detecting a phonon at time t, in the b_1 bosonic mode. As we can see from the figure that $g_{b1}^{(2)}(0) \approx 0$ but at any delayed time $\tau > 0, g_{b1}^{(2)}(\tau) > g_{b1}^{(2)}(0)$ for the plotted optimal values of $J/\gamma, U_{opt}$ and Δ_{opt}/γ and finally reaches the value 1. Therefore, it is evident that phonons are antibunched and have sub-Poissonian distribution. We observe that the antibunching behavior is sustained for a longer duration. As we increase the delay, the $g_{b1}^{(2)}(\tau)$ value eventually approaches 1 and becomes uncorrelated.

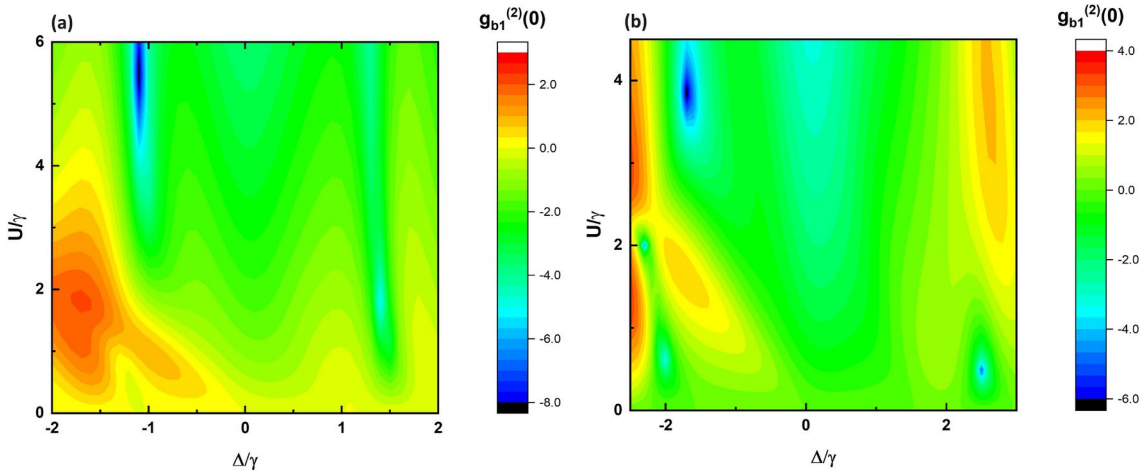

Fig. 5. Plot of $log_{10}(g_{b1}^{(2)}(0))$ as functions of normalized U and Δ for (**a**) $J/\gamma = 1.5$, and (**b**) $J/\gamma = 2.5$ Parameters: $\Omega = 0.01\gamma$.

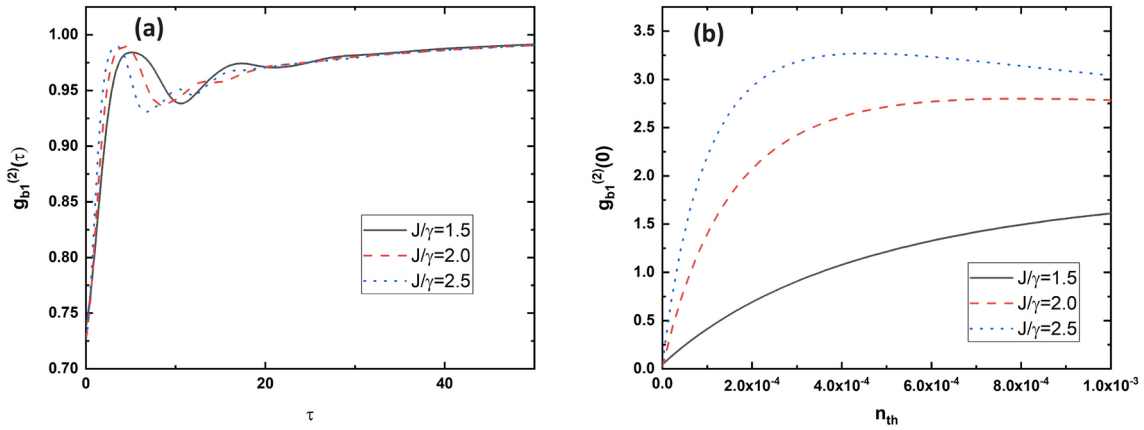

Fig. 6. (**a**) Plot of second order correlation function with finite time-delay $g_{b1}^{(2)}(0)$ as a function of delay τ. (**b**) Effect of environmental temperature on $g_{b1}^{(2)}(0)$. Parameters: $\Omega = 0.01\gamma$, $\Delta = \Delta_{opt}$ = 1.428, 1.995 and −2.30 and

Now, we plot $g_{b1}^{(2)}(0)$ as a function of phonon number, n_{th} in Fig. 6b to study the effect of environmental phonon population on the phonon blockade characteristic.For J/γ=1.5, $g_{b1}^{(2)}(0)$ reaches 1 at $n_{th} = 2.08 \times 10^{-5}$, whereas, for J/γ=2.0 and J/γ=2.5, $g_{b1}^{(2)}(0)$ remains below 1 up to $n_{th} = 6.12 \times 10^{-5}$ and $n_{th} = 3.47 \times 10^{-4}$ respectively. We can see that the environmental thermal population has a considerable unwanted effect on the phonon blockade characteristics.

Discussion

In summary, we have studied unconventional phonon blockade (UPB) in a system comprised of three coupled weakly nonlinear mechanical resonators. Phonon statistics are characterized in terms of second-order correlation functions. From the model Hamiltonian, we analytically derived the optimal conditions for achieving UPB in the proposed system. We also numerically studied the characteristics of UPB with zero time second-order correlation function, where we showed that by applying a single drive to one of the resonators, strong antibunching results for our proposed system at the optimum values of detuning and nonlinearity determined by our analytical derivation. Next, we studied the time-delayed second-order correlation function, where we found that the antibunching behavior was sustained for a longer duration until the phonons became uncorrelated. However, we saw that environmental phonons have a deleterious effect on phonon blockades. The most interesting finding of this study is the requirement of weak nonlinearity for the generation of phonon blockade effect. UPB with such weak nonlinearity is conducive for experimental realization of single phonon sources and thus can be crucial in quantum information and communication technologies.

Recently, there has been a growing interest in using carbon-based bottom-up devices due to their excellent mechanical and electrical properties. Carbon Nanotubes (CNT) based nonlinear resonators have been experimentally fabricated that approach quantum ground states[48]. These devices do not suffer excessive damping as their surfaces can be defect-free at the atomic scale. Thus, it is possible to fabricate carbon-based resonators that have very high quality factors and can operate at much higher frequencies[49–51]. These high frequency resonators relax the temperature required to achieve the ground state for the resonators, and thus, phonon blockade can be achieved at higher temperatures. The experimental realization of phonon blockade is still a challenge. While coupling between mechanical phonons and electromagnetic photons has been achieved in the quantum regime[52], the controlled coupling between multiple mechanical modes has so far been restricted to classical devices[53,54]. The challenge also lies in detection of antibunched phonon states that require ultra-strong coupling between the mechanical mode and optical mode for detection using photons: an elusive feat in optomechanics, though this has been achieved in related Quantum Electrodynamics (QED) experiments[55,56].

Methods

The optimal conditions for the phonon blockade can be determined by solving the set of evolution equations obtained from Schrodinger equation:

$$\begin{aligned}
i\dot{C}_{000} &= \Omega C_{001};\\
i\dot{C}_{100} &= (\Delta - i\frac{\gamma}{2})C_{100} + \Omega C_{000} + \sqrt{2}\Omega C_{200} + JC_{100};\\
i\dot{C}_{010} &= (\Delta - i\frac{\gamma}{2})C_{010} + \Omega C_{110} + JC_{100} + JC_{001};\\
i\dot{C}_{001} &= (\Delta - i\frac{\gamma}{2})C_{001} + \Omega C_{101} + JC_{010};\\
i\dot{C}_{200} &= 2(\Delta - i\frac{\gamma}{2} + U)C_{200} + \sqrt{2}\Omega C_{100} + \sqrt{2}JC_{110};\\
i\dot{C}_{110} &= 2(\Delta - i\frac{\gamma}{2})C_{110} + \Omega C_{010} + \sqrt{2}J\left(C_{020} + C_{200}\right) + JC_{101};\\
i\dot{C}_{002} &= 2(\Delta - i\frac{\gamma}{2} + U)C_{002} + \sqrt{2}JC_{011};\\
i\dot{C}_{011} &= 2(\Delta - i\frac{\gamma}{2})C_{011} + JC_{101} + \sqrt{2}J\left(C_{002} + C_{020}\right);\\
i\dot{C}_{101} &= 2(\Delta - i\frac{\gamma}{2})C_{101} + J\left(C_{011} + C_{110}\right) + \Omega C_{001};\\
i\dot{C}_{020} &= 2(\Delta - i\frac{\gamma}{2} + U)C_{020} + \sqrt{2}J\left(C_{011} + C_{110}\right)
\end{aligned} \tag{18}$$

In order to achieve UPB at resonator 1, the amplitude of $|200\rangle$ state must be suppressed. In the weak driving limit ($\Omega \ll \gamma$), the probability of excitation of phonons to higher energy levels becomes subsequently lower and thus we can assume $C_{000} \gg \{C_{100}, C_{010}, C_{001}\} \gg \{C_{200}, C_{110}, C_{020}, C_{101}, C_{011}, C_{002}\}$. The optimal condition for phonon blockade in the driven resonator then corresponds to the case when C_{200} vanishes. We solve the above set of equations under these assumptions to obtain the coefficients:

$$\begin{aligned}
C_{100} &= \frac{-\Omega\left((\Delta - i\frac{\gamma}{2})^2 - J^2\right)}{(\Delta - i\frac{\gamma}{2})\left((\Delta - i\frac{\gamma}{2})^2 - 2J^2\right)}C_{000};\\
C_{010} &= \frac{J\Omega}{\left((\Delta - i\frac{\gamma}{2})^2 - 2J^2\right)}C_{000};\\
C_{001} &= \frac{-J^2\Omega}{(\Delta - i\frac{\gamma}{2})\left((\Delta - i\frac{\gamma}{2})^2 - 2J^2\right)}C_{000};\\
C_{110} &= \frac{\Omega^2\left((\Delta - i\frac{\gamma}{2})^2 - J^2\right)}{J(\Delta - i\gamma/2)\left((\Delta - i\frac{\gamma}{2})^2 - 2J^2\right)}C_{000};\\
C_{011} &= \frac{-\sqrt{2}(\Delta - i\frac{\gamma}{2} + U)}{J}C_{002};\\
C_{101} &= \frac{-\Omega^2\left(2(\Delta - i\frac{\gamma}{2})^2 - J^2\right)}{J^2\left((\Delta - i\frac{\gamma}{2})^2 - 2J^2\right)}C_{000} - \sqrt{2}C_{020}
\end{aligned} \tag{19}$$

We substitute these to get three sets of equations for the unknown coefficients C_{000}, C_{020} and C_{002}. We then look for nontrivial solutions for which the determinant of the coefficient matrix must be zero. This gives us set of two equations, one for the real part and one for the imaginary part, solving which we obtain the set of optimal conditions for fixed values of coupling, J and damping rate, γ.

We then substitute the value of J and γ in the above equation to two equations for two unknowns, which can be numerically solved for optimal values for detuning Δ and nonlinearity U.

Data availability

The data that support the findings of this study are available from corresponding author upon reasonable request.

Received: 26 June 2024; Accepted: 19 September 2024
Published online: 06 October 2024

References

1. Henry Huang, X. M., Zorman, C. A., Mehregany, M. & Roukes, M. L. Nanodevice motion at microwave frequencies. *Nature* **421**(6922), 496–496 (2003).
2. Blencowe, M. Nanomechanical quantum limits. *Science* **304**(5667), 56–57 (2004).
3. Schwab, K. C. & Roukes, M. L. Putting mechanics into quantum mechanics. *Phys. Today* **58**(7), 36–42 (2005).
4. Ekinci, K. L. & Roukes, M. L. Nanoelectromechanical systems. *Rev. Sci. Instrum*. (2005).
5. Sarma, B. & Sarma, A. K. Tunable phonon blockade in weakly nonlinear coupled mechanical resonators via Coulomb interaction. *Sci. Rep.* **8**(1), 14583 (2018).
6. Miranowicz, A., Bajer, J., Lambert, N., Liu, Y. X. & Nori, F. Tunable multiphonon blockade in coupled nanomechanical resonators. *Phys. Rev. A* **93**(1), 013808 (2016).
7. Aspelmeyer, M., Kippenberg, T. J. & Marquardt, F. Cavity optomechanics. *Rev. Mod. Phys.* **86**(4), 1391 (2014).
8. Marquardt, F. Quantum optomechanics. Quantum Machines: Measurement and Control of Engineered Quantum Systems (Les Houches Session XCVI), edited by MH Devoret, B. Huard, RJ Schoelkopf, and LF Cugliandolo (Oxford University Press, 2014) (2011).
9. Rips, S. & Hartmann, M. J. Quantum information processing with nanomechanical qubits. *Phys. Rev. Lett.* **110**(12), 120503 (2013).
10. Habraken, S. J. M., Stannigel, K., Lukin, M. D., Zoller, P. & Rabl, P. Continuous mode cooling and phonon routers for phononic quantum networks. *New J. Phys.* **14**(11), 115004 (2012).
11. Aspelmeyer, M., Meystre, P. & Schwab, K. Quantum optomechanics. *Phys. Today* **65**(7), 29–35 (2012).
12. O'Connell, A. D. et al. Quantum ground state and single-phonon control of a mechanical resonator. *Nature* **464**(7289), 697–703 (2010).
13. Teufel, J. D. et al. Sideband cooling of micromechanical motion to the quantum ground state. *Nature* **475**(7356), 359–363 (2011).
14. Seis, Y. et al. Ground state cooling of an ultracoherent electromechanical system. *Nat. Commun.* **13**(1), 1507 (2022).
15. Nunnenkamp, A., Børkje, K. & Girvin, S. M. Single-photon optomechanics. *Phys. Rev. Lett.* **107**(6), 063602 (2011).
16. Rabl, P. Photon blockade effect in optomechanical systems. *Phys. Rev. Lett.* **107**(6), 063601 (2011).
17. Nation, P. D. Nonclassical mechanical states in an optomechanical micromaser analog. *Phys. Rev. A* **88**(5), 053828 (2013).
18. Bhatt, V., Barbhuiya, S. A., Jha, P. K. & Bhattacherjee, A. B. Nonlinear optical response properties of a quantum dot embedded in a semiconductor microcavity: possible applications in quantum communication platforms. *J. Mod. Opt.* **68**(4), 177–188 (2021).
19. Xu, X. W., Chen, A. X. & Liu, Y. X. Phonon blockade in a nanomechanical resonator resonantly coupled to a qubit. *Phys. Rev. A* **94**(6), 063853 (2016).
20. Wang, X., Miranowicz, A., Li, H. R. & Nori, F. Method for observing robust and tunable phonon blockade in a nanomechanical resonator coupled to a charge qubit. *Phys. Rev. A* **93**(6), 063861 (2016).
21. Liu, Y. X. et al. Qubit-induced phonon blockade as a signature of quantum behavior in nanomechanical resonators. *Phys. Rev. A* **82**(3), 032101 (2010).
22. Miranowicz, A., Paprzycka, M., Liu, Y. X., Bajer, J. & Nori, F. Two-photon and three-photon blockades in driven nonlinear systems. *Phys. Rev. A-Atomic Molecular Opt. Phys.* **87**(2), 023809 (2013).
23. Zhou, Y. H., Shen, H. Z. & Yi, X. X. Unconventional photon blockade with second-order nonlinearity. *Phys. Rev. A* **92**(2), 023838 (2015).
24. Majumdar, A. & Gerace, D. Single-photon blockade in doubly resonant nanocavities with second-order nonlinearity. *Phys. Rev. B-Condensed Matter Mater. Phys.* **87**(23), 235319 (2013).
25. Ma, Y. X. & Li, P. B. Deterministic generation of phononic Fock states via weak nonlinearities. *Phys. Rev. A* **108**(5), 053709 (2023).
26. Birnbaum, K. M. et al. Photon blockade in an optical cavity with one trapped atom. *Nature* **436**(7047), 87–90 (2005).
27. Faraon, A. et al. Coherent generation of non-classical light on a chip via photon-induced tunnelling and blockade. *Nat. Phys.* **4**(11), 859–863 (2008).
28. Hoffman, A. J. et al. Dispersive photon blockade in a superconducting circuit. *Phys. Rev. Lett.* **107**(5), 053602 (2011).
29. Xie, H., Liao, C. G., Shang, X., Ye, M. Y. & Lin, X. M. Phonon blockade in a quadratically coupled optomechanical system. *Phys. Rev. A* **96**(1), 013861 (2017).
30. Yin, T. S., Bin, Q., Zhu, G. L., Jin, G. R. & Chen, A. Phonon blockade in a hybrid system via the second-order magnetic gradient. *Phys. Rev. A* **100**(6), 063840 (2019).
31. Savona, V. Unconventional photon blockade in coupled optomechanical systems. arXiv preprint (2013).
32. Shen, H. Z., Wang, Q., Wang, J. & Yi, X. X. Nonreciprocal unconventional photon blockade in a driven dissipative cavity with parametric amplification. *Phys. Rev. A* **101**(1), 013826 (2020).
33. Liew, T. C. & Savona, V. Single photons from coupled quantum modes. *Phys. Rev. Lett.* **104**(18), 183601 (2010).
34. Gerace, D. & Savona, V. Unconventional photon blockade in doubly resonant microcavities with second-order nonlinearity. *Phys. Rev. A* **89**(3), 031803 (2014).
35. Lemonde, M. A., Didier, N. & Clerk, A. A. Antibunching and unconventional photon blockade with Gaussian squeezed states. *Phys. Rev. A* **90**(6), 063824 (2014).
36. Didier, N., Pugnetti, S., Blanter, Y. M. & Fazio, R. Detecting phonon blockade with photons. *Phys. Rev. B* **84**(5), 054503 (2011).
37. Ma, P. C., Zhang, J. Q., Xiao, Y., Feng, M. & Zhang, Z. M. Tunable double optomechanically induced transparency in an optomechanical system. *Phys. Rev. A* **90**(4), 043825 (2014).
38. Li, H. et al. Phonon blockade in a hybrid quadratically coupled optomechanical system. *Adv. Quant. Technol.* **7**(6), 2400034 (2024).
39. Xie, H., He, L. W., Shang, X. & Lin, X. M. Phonon blockade in a squeezed cavity optomechanical system. *Adv. Quant. Technol.* **7**(1), 2300239 (2024).
40. Liu, H. Y., Yin, T. S. & Chen, A. Magnetically Induced Two-Phonon Blockade in a Hybrid Spin-Mechanical System. *Magnetochemistry* **10**(6), 41 (2024).
41. Nema, J. K., Gupta, S., Thakkar, R. & Rajagopal, P. Novel hermetically sealed device to realize unconventional phonon blockade at near-micron dimensions and milliKelvin temperatures. *AIP Adv.* (2021).
42. Hensinger, W. K. et al. Ion trap transducers for quantum electromechanical oscillators. *Phys. Rev. A* **72**(4), 041405 (2005).
43. Chen, R. X., Shen, L. T. & Zheng, S. B. Dissipation-induced optomechanical entanglement with the assistance of Coulomb interaction. *Phys. Rev. A* **91**(2), 022326 (2015).
44. Navarrete-Benlloch, C. Open systems dynamics: Simulating master equations in the computer. arXiv preprint (2015).
45. Murch, K. W., Moore, K. L., Gupta, S. & Stamper-Kurn, D. M. Observation of quantum-measurement backaction with an ultracold atomic gas. *Nat. Phys.* **4**(7), 561–564 (2008).
46. Brennecke, F., Ritter, S., Donner, T. & Esslinger, T. Cavity optomechanics with a Bose-Einstein condensate. *Science* **322**(5899), 235–238 (2008).
47. Bamba, M., Imamoğlu, A., Carusotto, I. & Ciuti, C. Origin of strong photon antibunching in weakly nonlinear photonic molecules. *Phys. Rev. A* **83**(2), 021802 (2011).
48. Samanta, C. et al. Nonlinear nanomechanical resonators approaching the quantum ground state. *Nat. Phys.* **19**(9), 1340–1344 (2023).

49. Laird, E. A., Pei, F., Tang, W., Steele, G. A. & Kouwenhoven, L. P. A high quality factor carbon nanotube mechanical resonator at 39 GHz. *Nano Lett.* **12**(1), 193–197 (2012).
50. Huttel, A. K. et al. Carbon nanotubes as ultrahigh quality factor mechanical resonators. *Nano Lett.* **9**(7), 2547–2552 (2009).
51. Lassagne, B., Tarakanov, Y., Kinaret, J., Garcia-Sanchez, D. & Bachtold, A. Coupling mechanics to charge transport in carbon nanotube mechanical resonators. *Science* **325**(5944), 1107–1110 (2009).
52. Palomaki, T. A., Teufel, J. D., Simmonds, R. W. & Lehnert, K. W. Entangling mechanical motion with microwave fields. *Science* **342**(6159), 710–713 (2013).
53. Okamoto, H. et al. Coherent phonon manipulation in coupled mechanical resonators. *Nat. Phys.* **9**(8), 480–484 (2013).
54. Mahboob, I., Okamoto, H., Onomitsu, K. & Yamaguchi, H. Two-mode thermal-noise squeezing in an electromechanical resonator. *Phys. Rev. Lett.* **113**(16), 167203 (2014).
55. Niemczyk, T. et al. Circuit quantum electrodynamics in the ultrastrong-coupling regime. *Nat. Phys.* **6**(10), 772–776 (2010).
56. Yoshihara, F. et al. Superconducting qubit-oscillator circuit beyond the ultrastrong-coupling regime. *Nat. Phys.* **13**(1), 44–47 (2017).

Acknowledgements

This work is supported by Swarnajayanti Fellowship, Department of Science and Technology, India to the senior author, and Prime Minister's Research Fellowship, Government of India for the first author.

Author contributions

B.K. carried out theoretical and numerical calculations and P.R. supervised the project. All authors wrote and reviewed the manuscript.

Declarations

Competing interests

The authors declare no competing interests.

Additional information

Correspondence and requests for materials should be addressed to P.R.

Reprints and permissions information is available at www.nature.com/reprints.

Publisher's note Springer Nature remains neutral with regard to jurisdictional claims in published maps and institutional affiliations.